Published in : Journal of Chromatography A (2022), vol. 1677, 463208
DOI: 10.1016/j.chroma.2022.463208
Status : Postprint (Author's version)

QUANTIFICATION AND CHARACTERIZATION OF MINERAL OIL IN FISH FEED BY LIQUID CHROMATOGRAPHY-GAS CHROMATOGRAPHY-FLAME IONIZATION DETECTOR AND LIQUID CHROMATOGRAPHY-COMPREHENSIVE MULTIDIMENSIONAL GAS CHROMATOGRAPHY-TIME-OF-FLIGHT MASS SPECTROMETER/FLAME IONIZATION DETECTOR

Grégory Bauwens [a], Chiara Conchione [b], Nicola Sdrigotti [a,b], Sabrina Moret [b,*], Giorgia Purcaro [a,*]

[a] *Analytical Chemistry Lab, Gembloux Agro-Bio Tech, University of Liège, Passage des Déportés 2, Gembloux 5030, Belgium*
[b] *Department of Agri-Food, Environmental and Animal Sciences, University of Udine, via delle Scienze 206, Udine 33100, Italy*

KEYWORDS : Mineral oil saturated hydrocarbons (MOSH) ; Mineral oil aromatic hydrocarbons (MOAH) ; Comprehensive two-dimensional gas chromatography (GC × GC) ; Liquid-gas chromatography (LC-GC)

ABSTRACT

Mineral oil is an ubiquitous food contaminant potentially toxic. It is generally divided into aromatic hydrocarbons (MOAH) and saturated hydrocarbons (MOSH). These compounds are currently under investigation by the European Union to determine their occurrence and their toxicity before legislating on the matter. Although the discussion mainly focuses on food, animal feed can indirectly contribute to human exposure to such a contaminant.

In this study, seven commercial feeds were analyzed. The analyses were carried out in two different Universities (Udine-IT and Liège-BE), performing the same sample preparation protocol: microwave-assisted saponification and extraction followed by epoxidation for the MOAH fraction. The final determination was performed by hyphenated liquid-gas chromatography (LC-GC) and LC coupled to comprehensive multidimensional gas chromatography (LC-GC × GC) with parallel detection, namely flame ionization detector (FID) and time-of-flight mass spectrometer (ToFMS).

The results obtained by the two laboratories were generally in good agreement. The results obtained by LC-GC × GC-ToFMS/FID platform provided consistent results, with the advantages of more robust data interpretation that can compensate for problems occurring during purification. Moreover, the coupling of enhanced separation obtained by GC × GC and the MS information allowed for a more in-depth characterization of the contamination.

Published in : Journal of Chromatography A (2022), vol. 1677, 463208
DOI: 10.1016/j.chroma.2022.463208
Status : Postprint (Author's version)

1. Introduction

Mineral oil hydrocarbons (MOH) are petrogenic originated mixtures composed of a large number of isomers, which may contaminate foods via different routes. MOH is usually classified into MO saturated hydrocarbons (MOSH, including linear, branched, and alkyl-substituted cycloalkanes) and MO aromatic hydrocarbons (MOAH, including mainly alkyl-substituted (poly)aromatic hydrocarbons with a different number of fused rings) based on their chemical composition and toxicological relevance [1].

Although the occurrence of MOH has been known for about 30 years [2], the problem gained attention in 2008/2009, due to the finding of high levels of MOH in edible sunflower oil and paper-packed food (due to the migration from recycled paperboard fibers) [3,4]. As a result, in 2012 the European Food Safety Authority (EFSA) published an Opinion on MOH in food, highlighting the urgency of investigating further the occurrence of such a class of contaminants and stressing the lack of conclusive data for risk assessment [5]. Shortly after, the European Union (EU) required the collection of additional and more detailed occurrence data (Commission Recommendation 2017/84 [6]). More recently, the attention has been mainly focused on the most toxic fraction of the 3–7 ring MOAH [7]. In 2019 the Joint Research Center (JRC) published a Guidance recommending to follow a decision tree on whether to apply an additional purification step or not and defining the figure-of-merit of the method applied [8]. Both EFSA and JRC, suggested the use of comprehensive multidimensional chromatography (GC × GC) to clarify and support the interpretation of the results, as no mass spectrometer (MS)-based confirmatory method are available [5,8]. Despite the attempt of standardization in the JRC Guidance, lack of harmonized and validated protocols, lack of confirmatory methods, and the interpretation and integration of the final analytical data are still cumbersome issues that undermine the reliability of the data generated [9], [10], [11], [12]. Despite the reference analytical determination consisting of an advanced and wisely designed analytical determination using hyphenated liquid-gas chromatography-flame ionization detection (LC-GC-FID) [13], [14], [15], the GC chromatograms of MOSH and MOAH result in an unresolved complex mixture (UCM), generally called hump. The use of an FID for quantification purposes is required since it has a relative response factor of virtually 1 for both MOSH and MOAH. In contrast, the MS requires proper standards for calibration, which are not available [16]. The use of MS has been proposed in addition to the FID for quantification purposes, but not sufficiently selective fragments are formed; thus, it cannot rule out the presence of possible interferences [9,10]. Therefore, the use of the enhanced separation power provided by GC × GC has been suggested for an in-depth characterization and confirmation of MOSH and MOAH contamination [10,11,[17], [18], [19], [20], [21], [22].

The sample preparation protocol is also a critical step in determining the overall accuracy of the results. In fact, the sample preparation steps have to assure suitable extraction yield, enrichment, and purification, thus reaching adequate sensitivity while limiting procedural contamination. The JRC Guidance provides a useful decision tree to decide whether to apply an additional purification step to standardize the procedures among different laboratories, thus limiting the variability of the

Published in : Journal of Chromatography A (2022), vol. 1677, 463208
DOI: 10.1016/j.chroma.2022.463208
Status : Postprint (Author's version)

results. On the contrary, extraction and enrichment are often required, and no precise indications are provided on how to perform the extraction step.

In October 2018, the "Institut des Corps Gras & produits apparentés" (ITERG, Pessac, France), organized a collaborative trial for MOSH/MOAH determination. The method proposed was tested in an interlaboratory study via the analysis of both naturally contaminated and spiked samples (pre-mixtures, soybean meal, sunflower seeds, chicken feed, pig feed, vegetable oil) ranging from 3 to 286 mg/kg for MOSH and from 1 to 16 mg/kg for MOAH. This method involves a solvent extraction step with *n*-hexane, followed by epoxidation and on-line LC-GC-FID according to EN 16995, and is not suitable for encapsulated matrices. Fifteen laboratories out of 16 (representing 8 European countries) reported results, but the statistical evaluation was based on the results of 9 laboratories after eliminating the outliers. According to the precision data, considering as acceptable a value of 25% for the relative standard deviation (RSD), the method has been proven suitable for MOSH and MOAH concentrations equal or higher than 10 mg/kg. The validated method was recently published as EN 17517:2021 (Animal feeding stuff: Methods of sampling and analysis - Determination of MOSH and MOAH with on-line LC-GC-FID analysis).

Among the different methods proposed [23], [24], [25], [26] for MOSH/MOAH extraction/purification from complex food matrices, simultaneous microwave-assisted extraction and saponification appear to be the most promising in terms of throughput, efficiency, and solvent consumption [27,28].

In this context, the contamination of fish feed was investigated. Several studies in the literature have shown the accumulation of MOH in wild fish tissues, linking the finding to contaminated water (e.g., from oil spills) and biomagnification through the food chain [5,23,[29], [30], [31], [32], [33]. Scarce are instead the studies on farmed fish for which the primary source of contamination is represented by the feed, where MOH can be used for different purposes, such as binders for additives, to lubricate and reduce dustiness of pellets, to control the water content [5].

This work aimed to investigate and fully characterize the MOH contamination level (with particular emphasis to the MOAH) of feed intended for farmed fish. The results were validated by performing the analysis in two different laboratories (University of Udine, Italy, and Gembloux Agro-Bio Tech, Belgium) with different analytical platforms, namely an LC-GC-FID and an LC-GC×GC-FID/ToFMS. The latter platform has been proposed recently to merge the routine and confirmatory approach in a single analytical analysis [34]. In both laboratories, a rapid and solvent sparing protocol based on microwave-assisted saponification (MAS) was applied.

2. Material and methods

2.1. REAGENTS AND STANDARDS

Solvents were purchased from MilliporeSigma (Overijse, Belgium). The MOSH and MOAH internal standards (Restek #31070), containing 5-α-cholestane (Cho, 0.6 mg mL-1), *n*-C_{11} (0.3 mg mL-1), *n*-C_{13}

Published in : Journal of Chromatography A (2022), vol. 1677, 463208
DOI: 10.1016/j.chroma.2022.463208
Status : Postprint (Author's version)

(0.15 mg mL-1), cyclohexyl cyclohexane (CyCy, 0.3 mg mL-1), n-pentyl benzene (5B, 0.30 mg mL-1), 1-methyl naphthalene (1-MN, 0.30 mg mL-1), 2-methylnaphthalene (2-MN, 0.30 mg mL-1), tri-tert-butyl benzene (TBB, 0.3 mg mL-1) and perylene (Per, 0.6 mg mL-1) in toluene, and the MOSH/MOAH retention time standard, containing a standard mixture of *n*-alkane (C_{10}, C_{11}, C_{13}, C_{16}, C_{20}, C_{24}, C_{25}, C_{25}, C_{35}, C_{40}, and C_{50}), 50 mg/L each (Restek, #31076) were kindly provided by Restek (Neukirchen-Vlun, Germany). EPA 16 PAH and coronene (Cor) were from MilliporeSigma. 3-chloroperbenzoic acid (mCBPA), paraffin oil (hydrocarbon molecular range distribution comprised between n-C24 and n-C40), aluminum oxide, sodium thiosulfate, ethanol, n-hexane, dichloromethane were all from Merk-MilliporeSigma.

EXX-printing ink was kindly provided by a manufacturer. It is an offset printing ink with a hydrocarbon distribution between *n*-C_{14} and *n*-C_{20}, centered on *n*-C_{17} and with 20% of MOAH content. The Gravex solution used for sample spiking was kindly furnished by a producer. It consists of 73% of MOSH and 27% of MOAH in the range *n*-$C_{16–25}$.

The glassware was carefully washed and rinsed before use with distilled solvents (acetone and *n*-hexane).

2.2. SAMPLES

Seven commercial samples of fish feed intended for seabream (A and F), trout (B), marine fish (C, D and S), and seabass (E) were purchased from the Italian market.

Except for sample B, information given on the label were available. The different fish feeds had a fat content ranging from 15 (sample S) to 24% (sample E), sample A, C, and F had 16% of fat and sample D 21%. Except for sample C which contained vegetable oils only (soybean and rapeseed oils), all other samples contained fish oil, while sample E and F contained both fish and vegetable oils. Among other main ingredients, all contained fishmeal and various sources of vegetable protein (wheat gluten, wheat meal, rapeseed meal, sunflower meal, soybean meal or protein concentrate). None of the samples contained land animal proteins/oils or novel ingredients such as insect and algae meal or algae oil.

2.3. SAMPLE PREPARATION

Both laboratories, at the University of Udine (UniUD) and Gembloux Agro-Bio Tech (GxABT), applied the same sample preparation method involving a simultaneous saponification and extraction step assisted by the use of microwave (MAS) [28]. Briefly, saponification and extraction were carried out in an Ethos X microwave system equipped with a high-pressure SR 12 rotor from Milestone Srl (Milan, Italy) at the GxABT lab. The microwave extractor used at the UniUD lab was a Mars 5 from CEM Corporation (Matthews, North Carolina, USA), equipped with 14 GreenChem Plus Teflon. Five g of sample were directly weighed into a Teflon-lined vessel. Five µL of the IS mixture, 10 mL of saturated methanolic potassium hydroxide, and 10 mL of n-hexane were added. The vessel was sealed and positioned into the microwave extractor for 20 min at 120 °C as previously used for MOH extraction in cereal-based products [27]. After cooling, 40 mL of water followed by 2 mL of methanol were

Published in : Journal of Chromatography A (2022), vol. 1677, 463208
DOI: 10.1016/j.chroma.2022.463208
Status : Postprint (Author's version)

added, and the cell rested 30 min at −20 °C to facilitate phase separation. Finally, 5 mL of the n-hexane supernatant was withdrawn and concentrated to 1 mL. Of this, 300 µL were for direct MOSH analysis (except for sample B that underwent an auxiliary purification with alumina oxide according to the DGF protocol [35]), while the remaining 700 µL underwent epoxidation for MOAH analysis according to a slightly modified Nestola and Schmidt method [36]. Briefly, 500 µL of an ethanolic mCBPA 20% solution was added and the solution was stirred for 15 min at 500 rpm at room temperature. Then, 2 mL of aqueous sodium thiosulfate 10% solution and 500 µL of ethanol were added. The vial was shaken for 2 min. 500 µL of the n-hexane phase were transferred into an autosampler vial prefilled with a spatula tip of sodium sulfate and then injected into the LC-GC-FID system. All the samples were prepared in duplicates, and the results are provided as the average of the two determinations.

2.4. LC-GC-FID ANALYSIS

The analysis was carried out in the two laboratories using two different platforms. In UniUD an LC-GC-FID platform, while at GxABT, a fully automated LC-GC × GC-FID/TOFMS platform was used, both for the 1D and 2D analysis. Details of the two platforms are reported below. The performance of both platforms was constantly verified by assessing the MOSH and MOAH windows with the IS reference mixture (Restek #31070) and confirming that the response factor between *n*-C_{50} and *n*-C_{20} using the Restek MOSH/MOAH retention time standard (Restek, #31076) was between the accepted ration of 0.8 and 1.2 as required by the JRC Guidance.

2.4.1. LC-GC-FID UNIVERSITY OF UDINE (UNIUD)

On-line LC-GC-FID analysis was performed on a LC-GC 9000 from Brechbühler (Zurich, Switzerland). The LC column was 25 cm × 2.1 mm i.d. packed with Lichrospher Si 60, 5 mm (DGB, Schlossboeckelheim, Germany). The GC was a double channels Trace 1310 series from Thermo Scientific (Milan, Italy). Both channels consisted of a carrier gas line, Y-interface, retention gap, and GC column. The transfer of the LC fraction into the GC was carried out through a Y-interface [37], using the retention gap technique under the condition of partially concurrent eluent evaporation. A 10 m × 0.53 mm i.d. uncoated, deactivated precolumn was followed by a steel T-piece union connected to the solvent vapor exit and 15 m × 0.25 mm i.d. separation column, and coated with a 0.15 µm film of PS-255 (1% vinyl, 99% methyl polysiloxane; Mega, Italy). The FID (sampling frequency of 50 Hz) and solvent vapor exit were heated at 360 and 140 °C, respectively.

The LC gradient program was as follows: 0 min 100% n-hexane; 0.1–0.3 min reaches 30% dichloromethane. Flow rate at 300 µL/min. Six minutes after the injection, the column was backflushed with dichloromethane at 500 µL/min for 9 min and then reconditioned at 700 µL/min with hexane for 6.5 min and at 300 µL/min for 1.5 min.

The MOSH and the MOAH fractions were eluted from 2.0 to 3.5 min, and from 3.8 to 5.3 min, respectively.

GC program: from 55 to 350 °C at 20 °C/min and using hydrogen as carrier at a constant pressure of 60 kPa. During the transfer the pressure was increased to 90 kPa.

Published in : Journal of Chromatography A (2022), vol. 1677, 463208
DOI: 10.1016/j.chroma.2022.463208
Status : Postprint (Author's version)

2.4.2. LC-GC × GC-FID/TOFMS ANALYSIS UNIVERSITY OF GEMBLOUX AGRO-BIO TECH (GXABT)

The LC-GC and LC-GC × GC analyses were carried out in a fully integrated platform consisting of:

(1) An Agilent 1260 Infinity II LC equipped with an isocratic pump G7110B and a Variable Wavelength Detector acquiring at 230 nm (Agilent Technologies, Waldbronn, Germany). The pump was modified by Axel-Semrau to assure the minimization of the dead volumes.

LC conditions: A 250 mm × 2.1 mm i.d. × 5 µm d_p Allure silica column (Restek) was used. Solvent A was hexane and solvent B was dichloromethane. The gradient program was as follows: 0 min 100% A; 1.5–6 min 65% A at 0.3 mL/min. At 6.10 min the column was backflushed with 100% B for 9 min at 0.5 mL/min. The flow was then switched in forwarding mode to re-equilibrate the column with 100% hexane 10 min at 0.5 mL/min and 5 min at 0.3 mL/min until the following analysis.

(2) The LC and GC were connected through two rotatory switching valves (VICI AG International, Schenkon, Switzerland), to guide the LC eluent from the LC into the GC. The valves, the carrier gas, and the solvent vapor exit were controlled by CHRONECT LC-GC from Axel Semrau (Sprockhövel, Germany). The LC eluent was transferred into the GC through two on-column interfaces under the condition of partially concurrent eluent evaporation, using two parallel 10 m × 0.53 mm retention gap (siltek-treated retention gap from Restek) connected to two early solvent vapor exit (SVE) before the analytical columns. The system was equipped with two lines to transfer the MOSH and MOAH fraction simultaneously, one to the FID and the other to the MS. A scheme of the instrument is reported in Fig. 1.

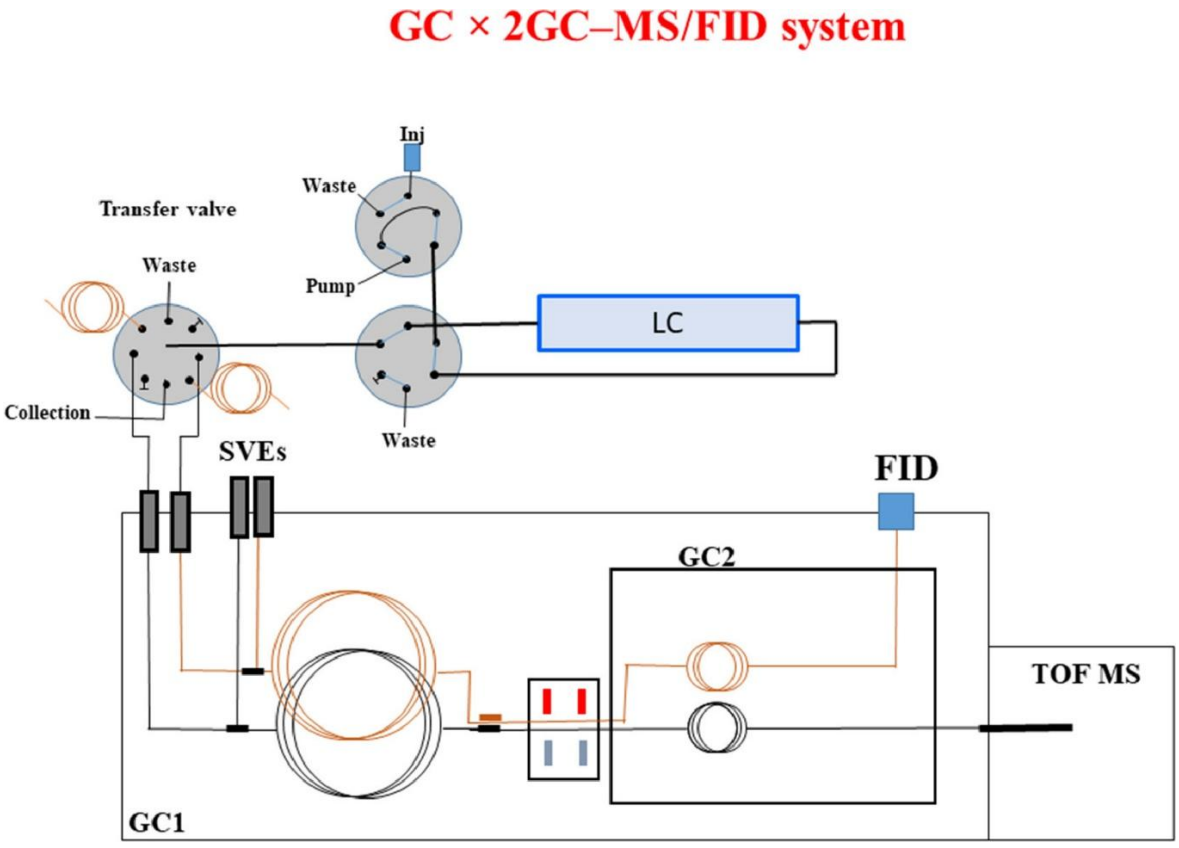

Fig. 1. Scheme of the LC-GC × GC-FID/TOFMS instrument.

Published in : Journal of Chromatography A (2022), vol. 1677, 463208
DOI: 10.1016/j.chroma.2022.463208
Status : Postprint (Author's version)

Transfer conditions: the MOSH fraction was transferred from the LC column between 2 and 3.5 min and the MOAH between 4.4 and 5.9 min (corresponding to 450 µL each). During the transfer, the inlet pressure was reduced from 130 to 110 kPa for MOSH and from 110 to 90 kPa for MOAH. The SVE was opened 0.5 min prior to transfer and closed 0.3 min after the transferring of the fraction.

(3) The GC and GC × GC system consisted of a Pegasus BT 4D GC × GC ToFMS (LECO, St. Joseph, MI, USA). The system is constituted by an Agilent 7890A gas chromatograph, equipped with a secondary oven and a quad-jet dual-stage thermal modulator, a time-of-flight (ToF) MS and an FID detector.

Both lines (to the FID and the MS) were equipped with a Rxi-65TG 15 m × 0.25 mm i.d. × 0.1 µm *df* connected to a Rxi-1 MS 2 m × 0.15 mm i.d. × 0.15 µm *df* (both from Restek).

GC oven temperature program for the 1D mode analysis: 60 °C (hold 8 min) to 350 °C (hold 5 min) at 20 °C/min. The modulator was switched off and a 5 °C positive offset (default setting), was applied for the modulator and the secondary oven.

GC oven temperature program for the 2D mode analysis: The 1D oven program of the primary oven was 60 °C (hold 8 min) to 350 °C (hold 5 min) at 8 °C/min. The secondary oven program was 100 °C for 11.67 min then 7 °C/min to 135 °C and finally 8 °C/min to 350 °C (hold 5 min). A 15 °C positive offset, was applied for the modulator.

The carrier gas, helium, was supplied in constant flow mode: 3.1 mL/min to the FID and 2.5 mL/min to the MS to compensate between the vacuum and the ambient pressure outlet. Modulation was performed every 10 s, applying variable hot and cold pulse durations based on the wide range of volatilities in the sample. The FID was operated as follows: H_2 flow: 30 mL/min; airflow: 300.0 mL/min; make up (He): 25.0 mL/min; Temperature: 360 °C. MS parameters: 50–700 *m/z*; spectra generation frequency (ToFMS and FID): 200 Hz in 2D and 20 Hz in 1D; MS interface and ion source temperatures were 340 °C and 250 °C, respectively. MS ionization mode: electron ionization (EI) at 70 eV.

Data was acquired and elaborated using the novel ChromaTOF Version 5 for MOSH/MOAH.

3. Results and discussion

3.1. METHOD VERIFICATION

Since it was not possible to find a clean sample, recovery tests were performed by fortifying with Gravex the sample with the lowest native contamination at two different fortification levels (7.5 and 18.8 mg/kg of total MOH, corresponding to 5.5 and 13.7 mg/kg of MOSH and 2.0 and 5.1 mg/kg of MOAH). The spiking levels reflect the range of the concentrations found in the analyzed samples. The sample used for recovery test had a pre-existing MOSH and MOAH contamination in the range *n*-C_{16-25} of 6.5 and 0.5 mg/kg, respectively.

Four aliquots of the selected sample weighted in the extraction cells were added with the known amounts of Gravex solution dissolved in 5 mL of pentane (containing 73% of MOSH and 27% of MOAH

Published in : Journal of Chromatography A (2022), vol. 1677, 463208
DOI: 10.1016/j.chroma.2022.463208
Status : Postprint (Author's version)

in the range *n*-$C_{16–25}$), and were gently stirred to uniformly distribute the mineral oil standard in the matrix. After aging the samples so prepared over the weekend in order to obtain analyte-matrix interactions and solvent evaporation, the samples underwent the entire procedure.

Percentage recoveries were calculated by comparing the amount found in the spiked samples, subtracted of the amount in the native sample (before the spiking), with that used to spike the samples.

Fig. 2 shows an overlay of the native sample before the spiking and of the sample at the two different fortification levels.

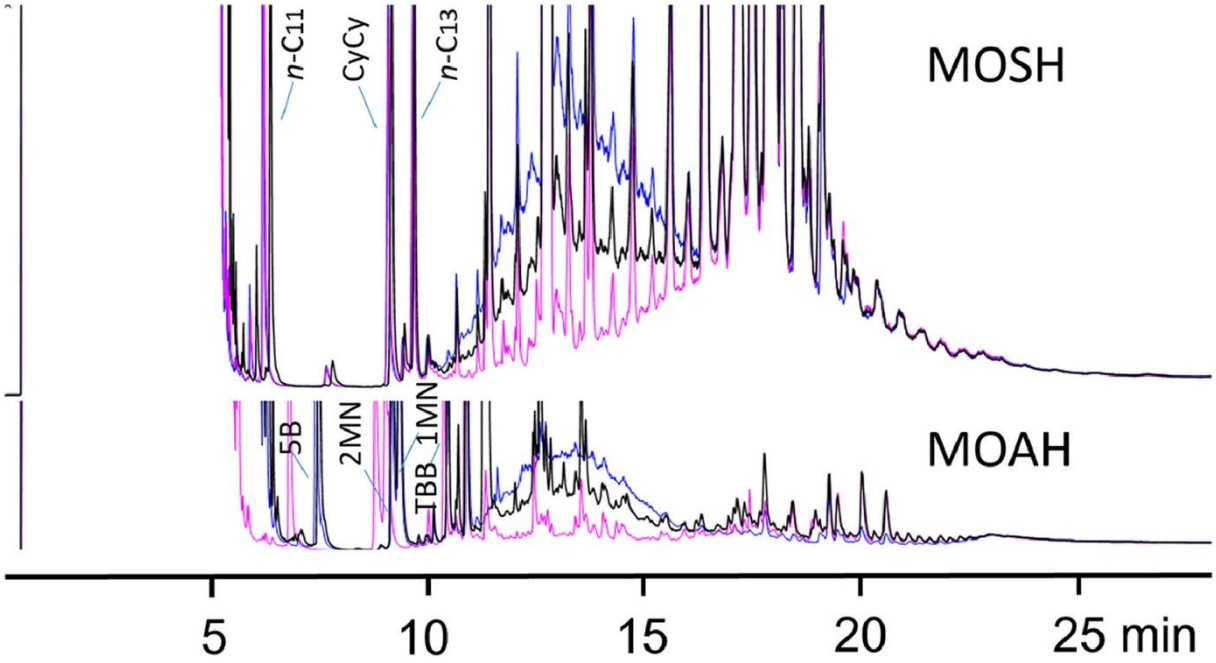

Fig. 2. LC-GC-FID chromatograms obtained applying the entire procedure to the native sample (pink trace), and the two level of spiking with Gravex, 7.5 mg/kg (black trace) and 18.8 mg/kg (blue trace).

Average MOSH recoveries (using CyCy as IS) were practically quantitative (104 and 105% for the lowest and the highest fortification level, respectively) with RSD < 6%. As reported by [38] for extra virgin olive oil, MOAH recovery varied depending on the IS used. This behavior is explained in more detail in the cited work and depends on the different partition observed when applying the saponification followed by hexane extraction. Practically quantitative recoveries were obtained when using 2MN as IS (on average 98 and 100% for the lowest and the highest fortification level, respectively) with RSD ≤ 8%. Average recoveries obtained with the other IS ranged from 78% when using TBB to 107% when using 1MN.

Repeatability was also assessed for each C-fraction, as requested by the JRC guidance [8], as well as for the total contamination in the range *n*-$C_{10–50}$. RSD not higher than 10% were obtained in all cases, also for C-fraction amounts around 0.5 mg/kg. These results were also confirmed by recovery tests at the lowest fortification level (4 replicate analyses).

The instrumental sensitivity of the LC-GC × GC-FID platform was assessed by building a calibration curve using five concentration levels (analyzed in triplicates in the 0.2–10.4 mg/kg range) of a

Published in : Journal of Chromatography A (2022), vol. 1677, 463208
DOI: 10.1016/j.chroma.2022.463208
Status : Postprint (Author's version)

mixture of paraffin and EXX-printing ink. The analyses were performed both in 1D and 2D modes. The standard deviation of the lowest concentration point was used to estimate the limit of quantification (LOQ) according to the equation $Y_{LOQ} = 10*SD_{b.}$ The values obtained for the two MOSH humps spread over different carbon ranges was averaged for the final LOQ estimation. A value of LOQ of about 0.1 and 0.05 mg/kg was calculated for 1D and 2D analysis, respectively (depending on the exact amount of sample injected).

3.2. DATA INTEGRATION

All the samples were analyzed on the two platforms and the results were compared. The MOSH and MOAH contents were reported, as required by the JRC Guidance, based on the C-fraction and the total MOSH and MOAH content in the *n*-C_{10}-C_{50} range [8]. CyCy and 2MN were used for MOSH and MOAH quantification, respectively, unless co-elution problems were detected.

3.2.1. UNIUD

The MOSH area was determined by integrating the whole hump of largely unresolved peaks, and subtracting the endogenous *n*-alkanes. All sharp peaks standing on the top of the MOAH "hump" were removed from the total area by manually integrating them and calculating the area of the resulting hump. The position of the baseline was assessed by procedural blank runs obtained on the same day.

3.2.2. GXABT

In GxABT, integration was performed using a novel algorithm that was developed on purpose for the particular problem of MOSH and MOAH integration [34]. The blank subtraction is automatically performed both in 1D and 2D by simply indicating the blank sample to use, thus significantly reducing the impact of the column bleed on the late eluted part of the chromatogram. The daily blank run was chosen for the corresponding samples run on the same day. Then, the well-shaped peaks riding on top of the hump are automatically trimmed based on a few parameters that the operator can define for each specified window and adjusted by visually controlling the resulting hump in both 1D and 2D. The 2D chromatograms can be inspected in 2D or 3D visualization or by creating a projection of the 2D separation on the x-axis, thus obtaining a reconstructed 1D hump for a more familiar interpretation of the trimming. The functioning of the automatic trimming is explained in detail in [34], and it is now incorporated into the commercial software used.

The integration of the 2D plot required an additional adjustment. In fact, a polar column in the first dimension and an apolar column in the second dimension were used. Therefore, a correction of the C-fraction windows was necessary; indeed, these are based on the elution of specific *n*-alkanes in an apolar column. In a polar column, *n*-alkanes are significantly less retained, thus changing the MOAH included in the C-fractions calculated based on the *n*-alkanes. The strategy to estimate the correction was the following: a mixture of 17 PAHs of different ring numbers was analyzed, and their linear retention indices (LRI) in the usual apolar column, like the one used in UniUD, and the polar column used in the LC-GC × GC-TOFMS/FID system, were compared (Fig. 3B). A well-defined linear

Published in : Journal of Chromatography A (2022), vol. 1677, 463208
DOI: 10.1016/j.chroma.2022.463208
Status : Postprint (Author's version)

correlation (R^2 = 0.9985) was observed (Fig. 3A); therefore, the regression equation (i.e., y = 1.2494x-118.85) was used to calculate the corrected LRIs in the polar column (and consequentially the retention times) to define the MOAH C-fractions as indicated by the JRC Guidance. So, for instance, the C_{10}-C_{16} fraction, which corresponds to the 1000–1600 LRI range, once converted in the polar elution retention window for MOAH, corresponded to 1131–1880 LRI range. In the 2D plot, the classification areas for each C-fraction were drawn taking into account the apolar nature of the compounds eluted on the top part of the 2D plot and the more polar nature of the one eluted on the lower part; thus, for instance, the C_{10}-C_{16} fraction was delimited by 1000 and 1600 in the upper part, but by 1131 and 1880 in the lower part, obtaining a trapezoidal shape of the C-fraction (Fig. 3C). It is important to highlight that the retention shift of the MOAH may change based on the extent of alkylation and a more in-depth investigation would be necessary to evaluate it. Nevertheless, considering that observing the two chromatograms reported in Fig. 3B the shift in retention times is more significant for the *n*-alkane rather than for the PAHs, it can be concluded that the correction performed is a good estimation of the shift of the entire class of compounds in the defined C-fraction.

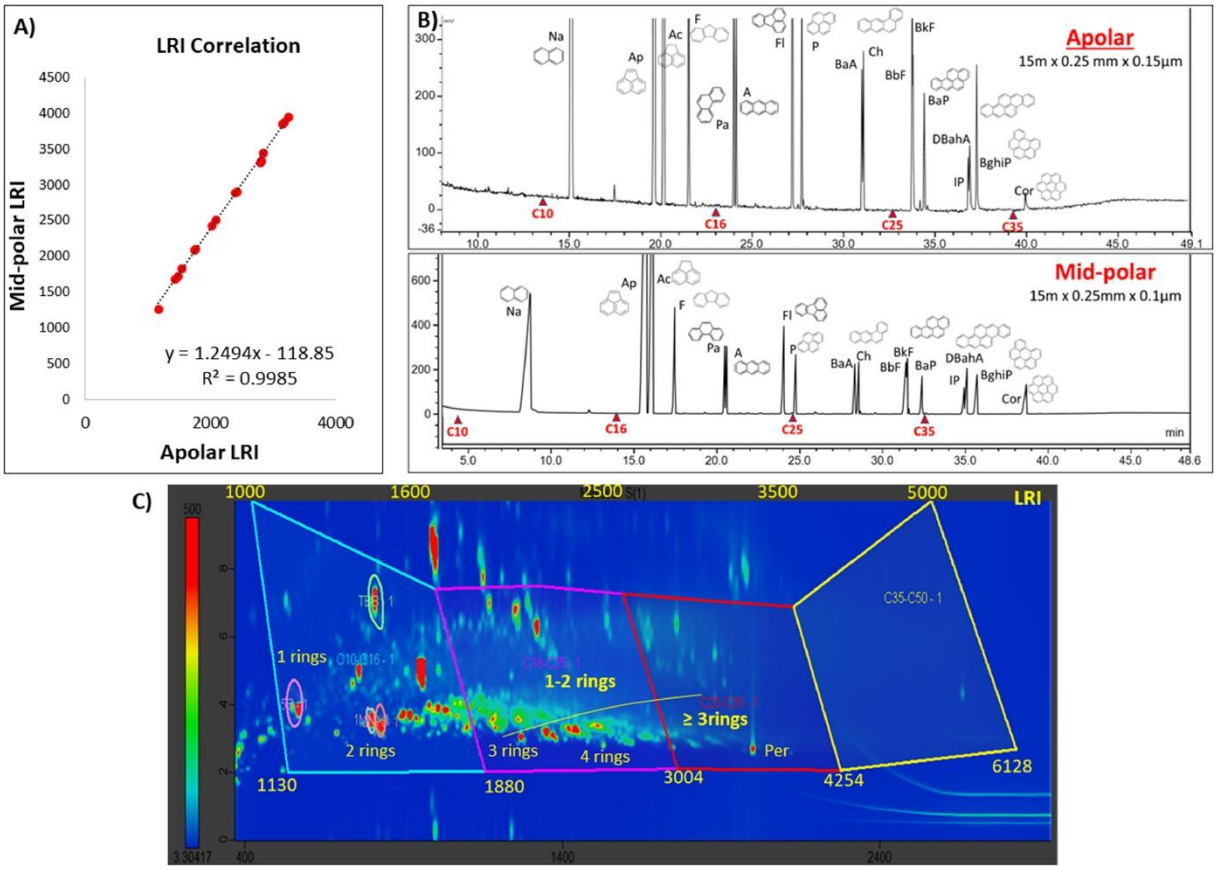

Fig. 3. (**A)** Regression correlation between the LRI calculated for each PAH (represented by the red dot) on the Apolar column (x-axis) and the polar column (y-axis); (**B)** comparison of the retention behavior in the apolar and mid-polar column. Red triangles indicate the elution of the C_{10}, C_{16}, C_{25}, and C_{35} n-alkanes; acenaphtene (Ac), fluoranthene (Fl), naphthalene (Na), benzo(a)anthracene (BaA), Benzo(b)fluoranthene (BbF), benzo(a)pyrene (BaP), benzo(k)fluoranthene (BkF), chrysene (Ch), acenaphthylene (Ap), anthracene (A), benzo(g,h,i)perylene (BghiP), fluorene (F), phenanthrene (Pa), pyrene (P), dibenz(a,h)anthracene (DBahA),

Published in : Journal of Chromatography A (2022), vol. 1677, 463208
DOI: 10.1016/j.chroma.2022.463208
Status : Postprint (Author's version)

indeno(1,2,3-cd)pyrene (IP), and coronene (Cor); **C)** 2D plot for the MOAH fraction with the adjusted integration for the polar × apolar column set.

3.3. LC-GC × GC-TOFMS/FID DATA INTERPRETATION

The fully integrated LC-GC × GC-FID/MS platform provided a series of extra information, thanks to the enhanced separation power, which acts as an additional sample preparation step for some classes of compounds, and the extra MS dimension.

3.3.1. THE MOSH FRACTION

On the MOSH fraction, a clear separation of sterane and hopanes, markers of petrogenic origin (Supplementary Fig. S1) [39,40], can be observed without the need for the higher sensitivity provided by the ToFMS detector. In fact, when the concentration of MOSH is sufficiently high, they can easily be spotted in the FID plot chromatographically separated by the rest of the MOSH.

The expected pattern in the 2D plot, reflecting a clear chemical class separation that can be drawn using regular lines, showed an unregular behavior in the early part of the chromatogram, showing an increasing and then suddenly decreasing trend around 800 s of the first dimension retention time. This was due to the long isotherm period required to perform the concurrent solvent eluent evaporation to transfer the 450 µL from the LC into the GC in an efficient way. Therefore, to reduce the impact of this isotherm on the class pattern distribution, an adapted secondary oven program was applied starting from a higher offset (+40 °C) with a longer isotherm (11.67 min rather than the 8 min of the primary oven) then the temperature of the primary oven increased at 8 °C/min, while the secondary oven increased slightly slower, at 7 °C/min to 135 °C and then followed the temperature ramp of the primary oven with an offset of about +5 °C.

3.3.2. THE MOAH FRACTION

Regarding the MOAH fraction, several considerations can be made. Firstly, the use of 0.1 µm stationary phase thickness (d_f) in the first dimension column provided an overall earlier elution time, which means at lower elution temperature that reflects in a better separation of the sub-classes in the second dimension compared to the widely used 0.15 µm d_f. The MOAH with different aromatic ring numbers are well separated in the 2D space, and, in particular, the monoaromatics are more spread in the 2D plot. It can also be observed in Fig. 3 (and better in the expansion of Supplementary Fig. 2A and B), the clear separation of the so called "2.5-rings" (i.*e.*, partially hydrogenated MOAH as acenaphthene) from the 2-rings and the 3-rings. Such a separation is less evident in the 2D chromatograms reported in the literature using the most common mid-polar 50% phenyl 1D column. The separation between the groups of 4-rings as pyrene (P) and fluoranthene (Fl) versus the benzo(a)anthracene (BaA) and chrysene (Ch) is also clearly present.

In the samples analyzed, the presence of two clusters of peaks can also be observed, forming two small humps in the upper-right part of the 2D plot (circle in Fig. 4A). This part of the TIC chromatogram is shown in an expansion in Fig. 4B. In the circle noted as 1, squalene was clearly identified extracting the fragment ion 137 *m/z;* while slightly less retained, there were a series of

Published in : Journal of Chromatography A (2022), vol. 1677, 463208
DOI: 10.1016/j.chroma.2022.463208
Status : Postprint (Author's version)

compounds characterized by a high intensity of fragment 253 *m/z* (Fig. 4C). This specific fragment ion, as well as the relative retention of the compounds characterized by this fragment (just slightly more polar than squalene), were previously reported by Biedermann et al. [41], and, despite an explanation on the structure providing such fragment was not found, it was hypothesized that they were related to epoxidation-resistant squalene derivatives.

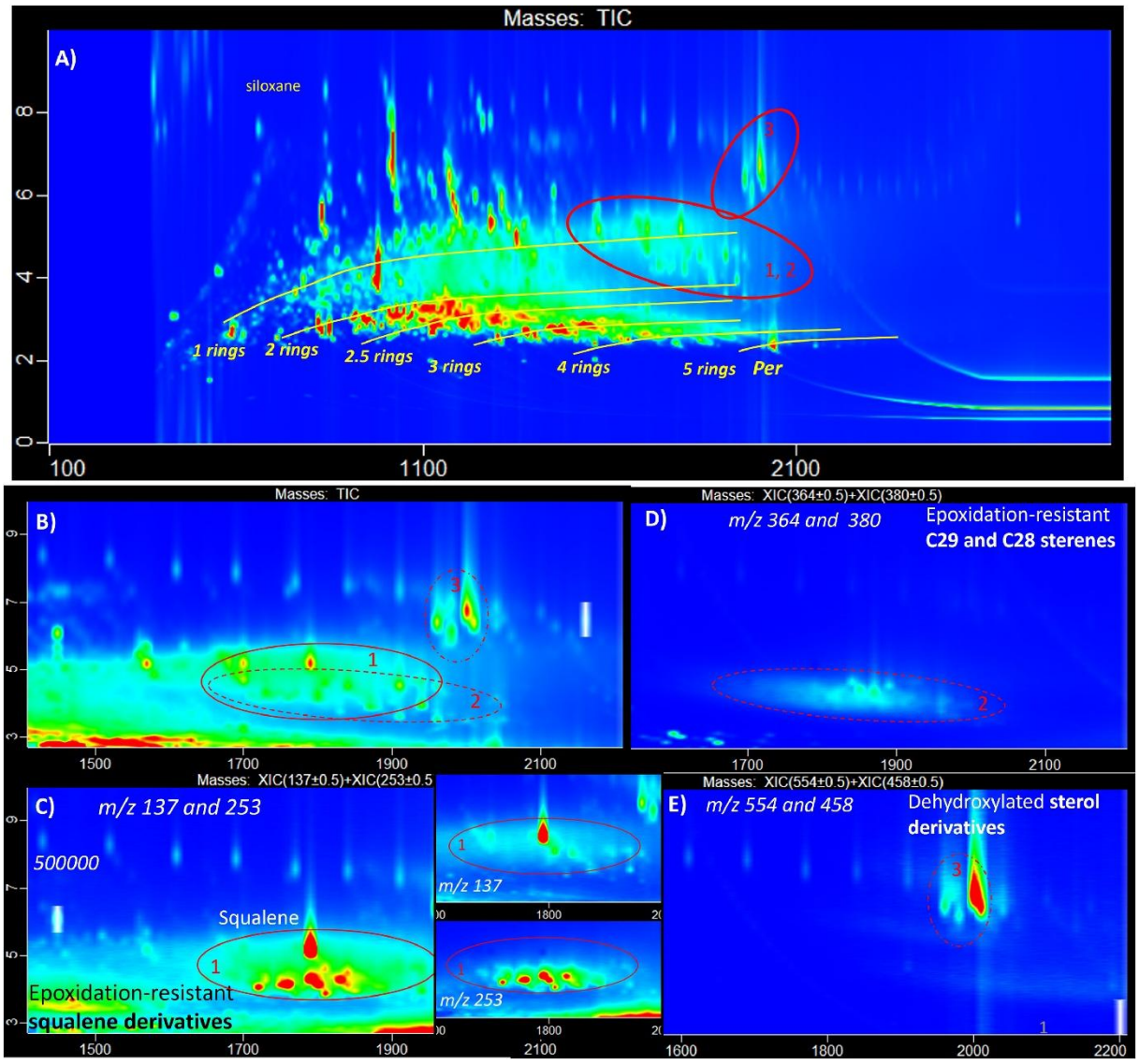

Fig. 4. (**A)** Total Ion Current (TIC) 2D chromatogram of sample S obtained by LC-GC × GC-ToFMS. (**B)** Expansion of the area containing compounds circled as 1,2, and 3. (**C), (D),** and (**E)** extracted ions chromatograms corresponding to *m/z* 137 and 253, 364 and 380, and 554 and 458, respectively.

Within the circle noted as 2, fragments 364 and 380 *m/z* were detected. These two fragments, along with the 2D position, were correlated to the presence of non-epoxidized C29 and C28 sterenes [41]. For one of the signals, the library suggested (3β)-Cholesta-4,6-dien-3-ol, with a similarity > 800, the characteristic fragments, i.e., 366 and 143 *m/z* were present, but a lower intensity than expected was observed for the 247 *m/z* fragment ion. The deviation from the expected spectrum along with the consideration that sterols are not eluted from the LC chromatographic column in the MOAH fraction

Published in : Journal of Chromatography A (2022), vol. 1677, 463208
DOI: 10.1016/j.chroma.2022.463208
Status : Postprint (Author's version)

suggested the presence of C28 sterenes (though not necessarily from dienes). In the same zone (zone 2), co-elution of carotenoid derivatives was observed with similarities over 800 for some peaks but with an overall very low intensity.

The compounds within the circle identified as 3 eluted slightly above the monoaromatic zone of the 2D plot, thus suggesting a less polar nature of these compounds and a different chemical structure compared to the MOAH sub-fraction. Although at very low intensity, the 554 and 458 *m/z* fragments were reported as possibly the molecular ions. No library match with sufficient similarity was observed, but it may be hypothesized that some dehydroxylated sterol-derivatives may be present **(**Fig. 4E). Anyway, the contribution of these compounds is chromatographically removed from the quantification of the MOAH when using the 2D GC separation, thus reducing the uncertainty linked to the integration process of the riding peaks and the remaining contribution they would provide. This is also true for the many interfering peaks eluted above the monoaromatic zone in the earlier part of the 2D chromatogram. The identification is cumbersome because the similarities with the MS database are very low but generally suggest the presence of an unsaturated linear carbon chain (with an unsaturation degree below the squalene but enough to be eluted in the MOAH fraction rather than the MOSH, thus justifying the increased retention in the 2D column).

In all the MOAH fractions, a particular cluster of well-shaped peaks was observed in the monoaromatic area of the chromatogram. These compounds were further investigated using the ToFMS trace and they were characterized as long-chain alkylbenzenes (LABs) with C_{10}-C_{13} aliphatic chain. For the C_{10}-LAB only the 2 positional isomer (C_{10}-LAB-2, which means that the aliphatic chain is linked to the benzene ring through the second carbon of the 10-C chain, as illustrated in the box of Fig. 5C) was detected. Whether other C_{10}-homologous might be present is difficult to determine due to the intense interference of BHT (butylhydroxytoluene) coeluted nearby the C_{10}-homologous in all the samples.

The entire range of isomers, with the alkyl chain linked to the position 2 to 6 to the benzene ring, were detected for the C_{11}-C_{13}-LABs [42], [43], [44], [45], [46]. The elution order of the isomers within the C-group is the C*n*-LAB-6 eluted first and the C*n*-LAB-2 isomer eluted the last. The LABs pattern was characterized by the 91 *m/z* base peak fragment ions for the C*n*-LAB-3–6, deriving from the cleavage of the benzylic bond, and the following characteristic fragments: 119, 133, 147, 161 *m/z* fragments for the positional isomers from 3 to 6, respectively. In contrast, the 105 *m/z* fragment ion was the base peak for all the C*n*-LAB-2 congeners. The molecular ions were also detected being fragment ions 218, 232, 246, 260 *m/z* for the C_{10}-, C_{11}-, C_{12}-, C_{13}-LABs, respectively. Fig. 5 shows the LC-GC × GC-ToFMS trace of sample A where a high contribution of LABs was detected (over 13%), along with an expansion of the TIC signal and the extracted ion of 105 *m/z* to delimit the different families of C*n*-LABs.

Published in : Journal of Chromatography A (2022), vol. 1677, 463208
DOI: 10.1016/j.chroma.2022.463208
Status : Postprint (Author's version)

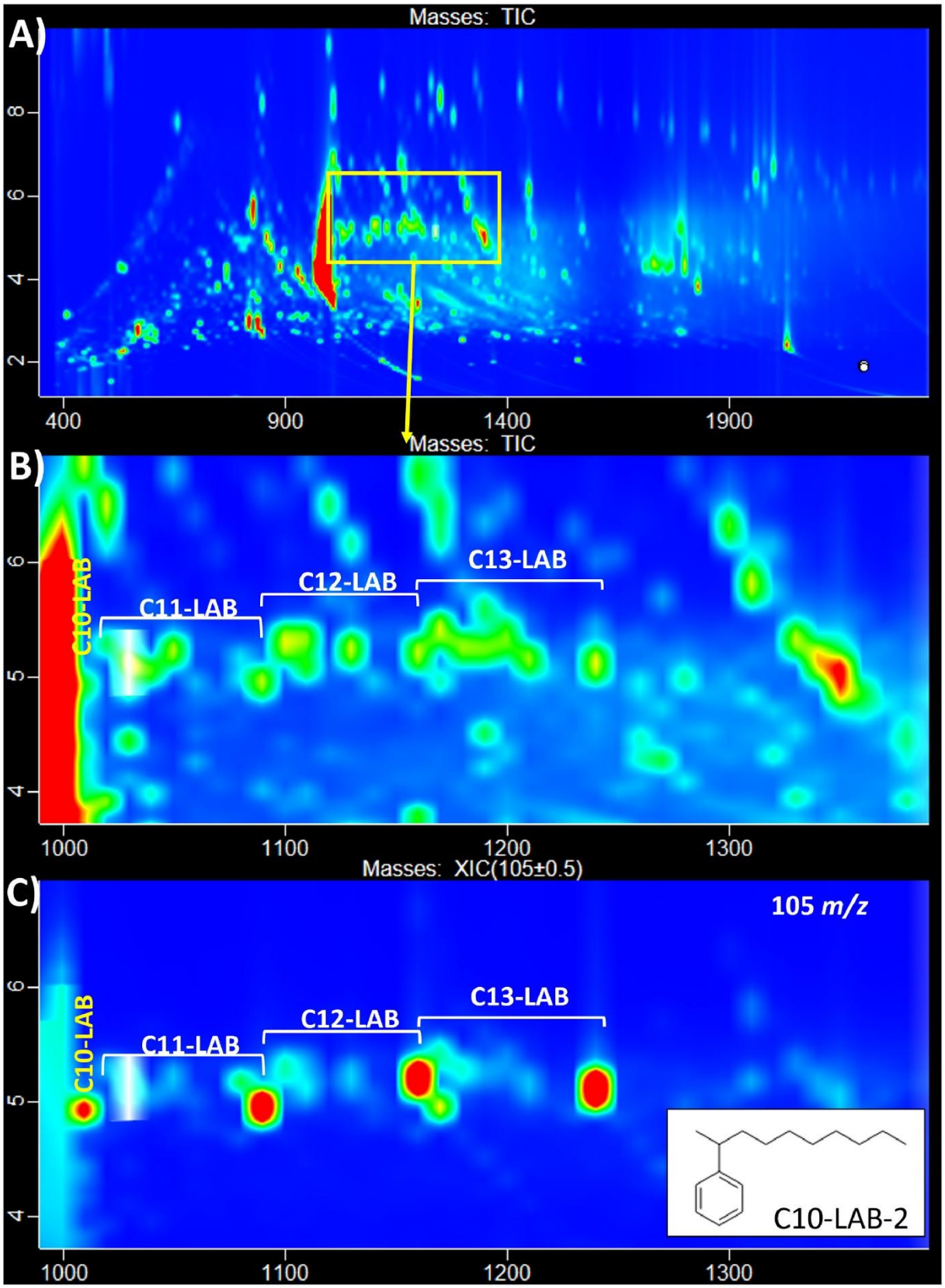

Fig. 5. (**A)** Total Ion Current (TIC) 2D chromatogram of sample A obtained by LC-GC × GC-ToFMS. (**B)** Expansion of the area within the rectangle in A. (**C)** Extracted ion (*m/z* 105) 2D chromatogram highlighting the presence of the Cn-LABs-2 isomers of the C10-, C11, C12, and C13-LABs families. In the box the structure of C10-LABs-2.

Published in : Journal of Chromatography A (2022), vol. 1677, 463208
DOI: 10.1016/j.chroma.2022.463208
Status : Postprint (Author's version)

LABs have been detected in marine sediments, and they have been related to municipal waste. LABs are the raw material for the synthesis of alkylbenzene sulfonate surfactants which are synthesized in two steps: (I) alkylation of benzene using linear C_{10} to C_{14} olefin or chloroparaffin chains; (II) sulfonation of the benzene ring. The incomplete sulfonation of benzene during the last step leads to the residual presence of LABs, which persist in the final detergent [46]. The fish feed samples can have entered in contact with surfactants from different sources, such as during processing or migration of residues from packaging used for the final product or of one or more ingredients [44,47]. However, the predominance of the C_{11} to C_{13} homologous and the depletion of the C_{14}-homologous may suggest bioaccumulation of these products in the fish tissue used as an ingredient of the final feed, consistently with the profiles previously found in fish tissue [28,42,45,48].

Finally, in all the samples, traces of PCB were also detected (Fig. 6), eluted between the diaromatics and the triaromatic. Despite a good similarity obtained at the MS (over 800), the elution of the PCB from the LC column in the MOAH fraction has never been reported before. Therefore, a verification with standards would be needed to confirm the finding. It would be interesting in the future to investigate further the capability of the proposed platform to monitor the presence of both contaminants.

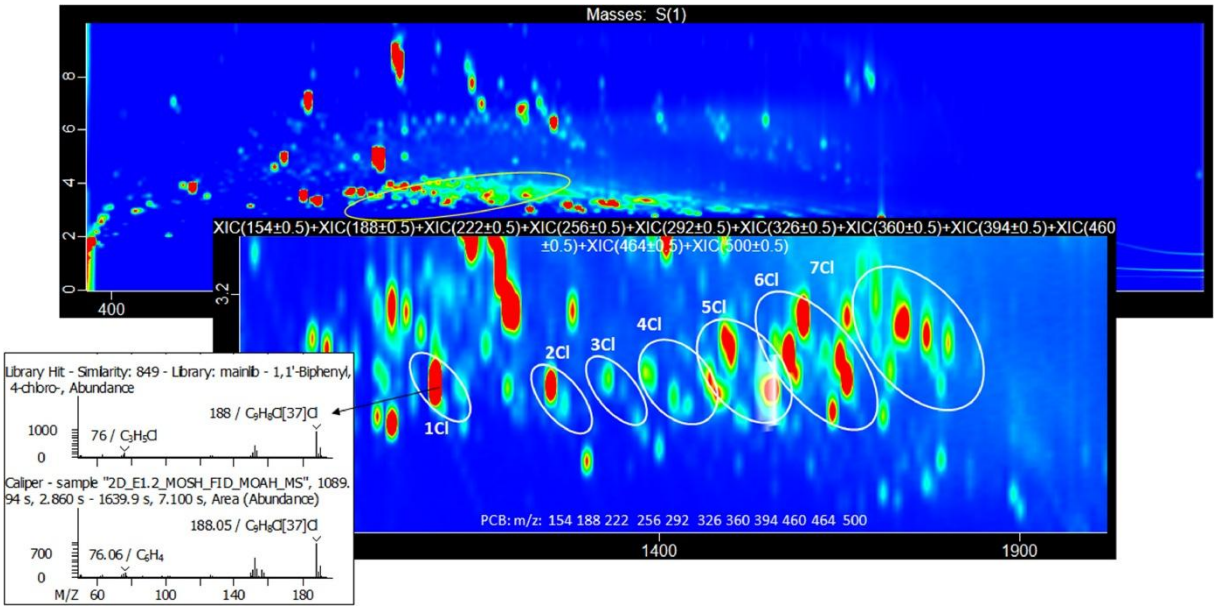

Fig. 6. Extracted ion chromatogram (XIC, *m/z* 154, 188, 222, 256, 292, 326, 360, 394, 460, 464, 500) of the expansion of the chromatogram where the PCB are eluted. The circle indicates the number of chloride substitutes in the biphenyl molecule. An example of the library match for 1 Cl-PCB is also reported.

3.4. MOSH AND MOAH CONTENT IN COMMERCIAL FISH FEED SAMPLES

All the samples were prepared separately at UniUD and GxABT, following precisely the same protocol but with different analytical instruments.

MOAH were quantified using 2MN, since it provides the most consistent recovery after microwave-assisted saponification (MAS). The total amount of MOSH and MOAH in the *n*-C_{10-50} range are reported

Published in : Journal of Chromatography A (2022), vol. 1677, 463208
DOI: 10.1016/j.chroma.2022.463208
Status : Postprint (Author's version)

in Fig. 7A and B, while the distribution for the different C-fractions is reported in Supplementary Fig. 3.

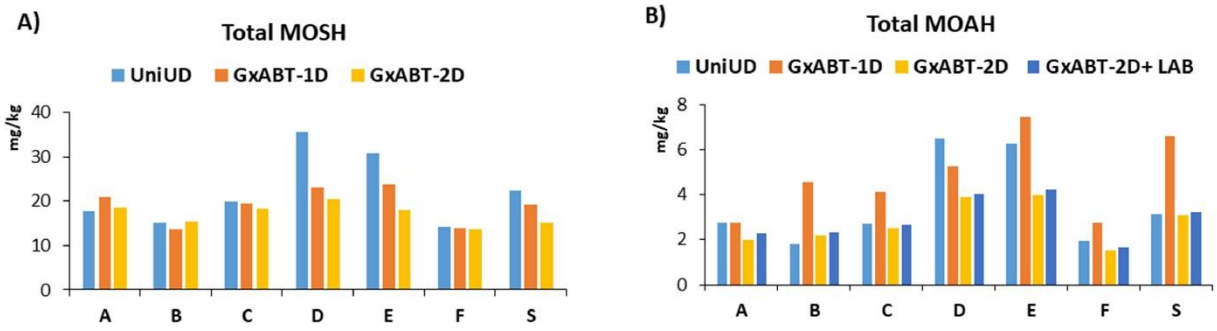

Fig. 7. Total (**A)** MOSH and (**B)** MOAH content of the fish feed samples obtained by the LC-GC-FID analysis at UniUD, and by the LC-GCxGC-FID analysis performed without modulation (orange bars) and with modulation (yellow bar) by GxABT. Moreover the results added by the LABs contribution are reported in the case of GxABT in reference to the 2D quantification.

Although the number of samples is too low to make a correlation, it can be observed that samples D and E, which had the highest fat content (21 and 24%, respectively), also had higher MOSH and MOAH contamination with respect to other fish feeds, whose fat content ranged from 15 to 16%. The MOSH results were generally in good agreement between the two laboratories and the different analyses performed, with a variation in the 2.0–18.8% range (expressed in RSD%) among the 3 results (i.e., 1D UniUD, 1D and 2D GxABT). Exceptions are samples D and E for which variability of 30.6% and 26.3% were observed, respectively.

The 7 fish feed samples showed very similar MOSH profiles with an enlarged asymmetrical hump (in some cases clearly formed by two different humps) starting from *n*-C_{14} to up to *n*-C_{50}, with a maximum generally around *n*-C_{30}.

It is interesting to observe as all samples showed in the first part of the MOSH trace some peaks, among which prevailed *n*-C_{17}, followed by *n*-C_{15}, *n*-C_{19}, *n*-C_{16}, *n*-C_{18}, and *n*-C_{14}, which probably derive from the fishmeal (which generally contains 9–11% of fat) and/or the fish oil used as an ingredient. Indeed, it is well known that fish may bioaccumulate a huge amount of these *n*-alkanes from the aquatic environment.

Fig. 8 compares the LC-GC-FID chromatograms of the MOSH and MOAH fractions of fish feed D and a fish fillet (wild salmon) analyzed in UniUD lab a couple of years ago.

Published in : Journal of Chromatography A (2022), vol. 1677, 463208
DOI: 10.1016/j.chroma.2022.463208
Status : Postprint (Author's version)

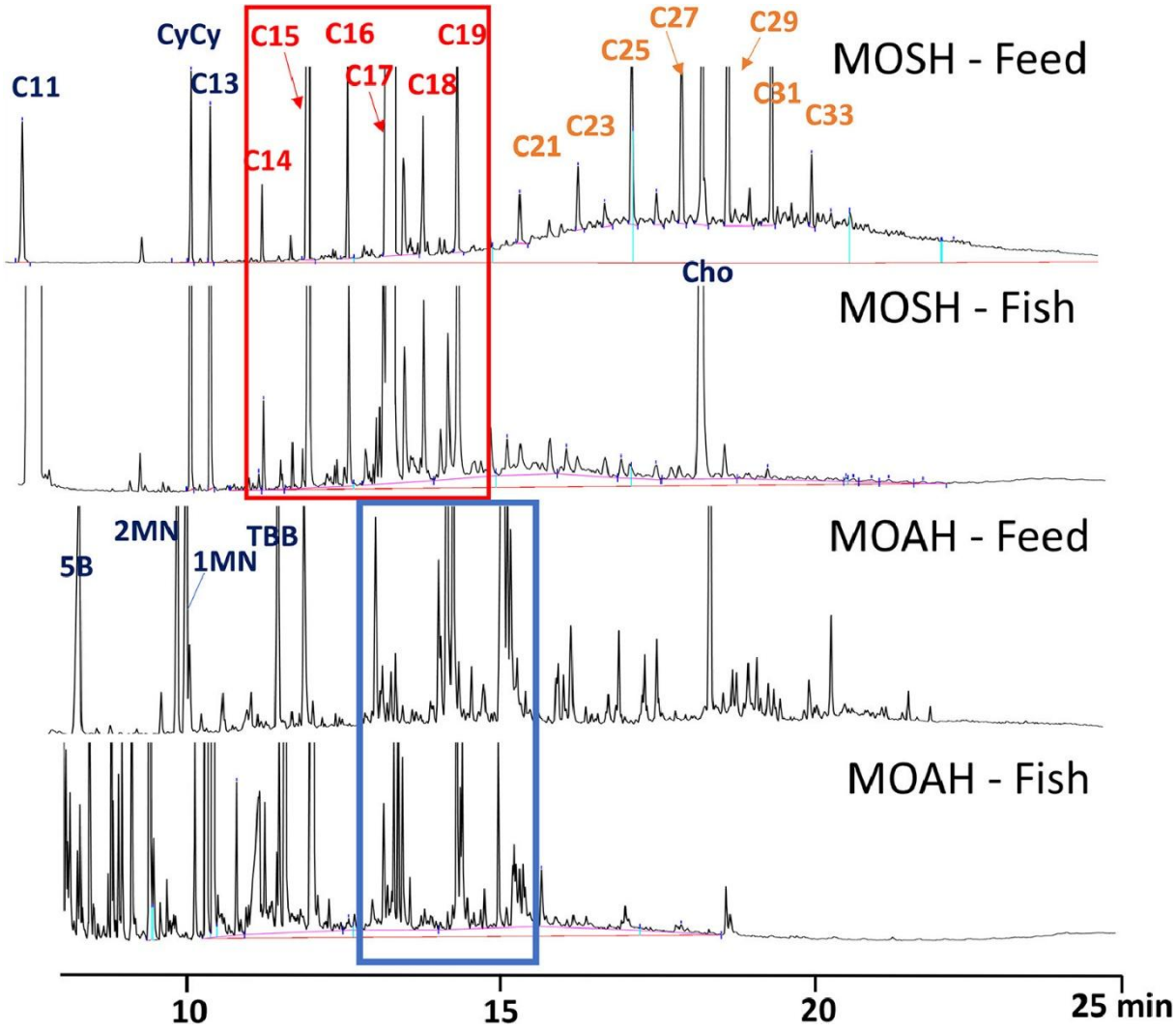

Fig. 8. Comparison of the LC-GC-FID chromatograms of the MOSH and MOAH fractions of fish feed D and of a fish fillet (wild salmon) analyzed in Uniud lab a couple of years ago. On the upper chromatograms (MOSH fractions) highlighted in red the common hydrocarbons between the feed and the fish samples. In the bottom chromatograms (MOAH fractions) highlighted in blue the common interferences between feed and fish.

It is well evident as endogenous *n*-alkanes in the range *n*-C_{14}-C_{19} are also present, with the same prevalence of the feed, in the fish fillet, whereas in the fish fillet, there is no evidence of the presence of *n*-alkanes in the range *n*-C_{21}-C_{33}, present in all the feed samples. Such *n*-alkanes are typical of vegetable oils but could also be present in fish oil.

Surprisingly, we found no differences in the *n*-alkane composition of the feed that contained exclusively vegetable oil (in this case, the fish meal was the first ingredient) and those that contained both vegetable and fish oil, or only fish oil. All the samples had a very similar *n*-alkane composition, where the most abundant *n*-alkane was *n*-C_{29}, followed by *n*-C_{31}, *n*-C_{27} and *n*-C_{25} (the last two being present approximately at the same concentration). Looking at the MOAH results, the variability among the 1D and 2D results determined by UniUD and GxABT is higher. The MOAH content determined in 1D by GxABT is generally higher than the result reported by UniUD (except for sample A), while the quantifications performed on the 2D data agreed with the results of UniUD (except for

Published in : Journal of Chromatography A (2022), vol. 1677, 463208
DOI: 10.1016/j.chroma.2022.463208
Status : Postprint (Author's version)

sample D and E). A general lower trimming of the interference peaks from the main hump due to the automate process, as observed in the 1D traces comparison of Fig. 9 and Supplementary Fig. S4 can be observed in the case of the 1D analysis at GxABT. The 2D results, instead, showed a lower overall quantification of the MOAH fraction compared to the 1D results at GxABT, this is due to the fact that many compounds are chromatographically separated from the MOSH and MOAH fractions thus limiting the overestimation of the contamination due to a lower trimming of the riding peaks, which is highly affected by the operator interpretation. For instance, compounds circled as 3 in Fig. 4A and all the earlier eluted compounds eluted above the monoaromatic fraction are excluded from the zone of the integration without the need to subtract them from the overall area, thus reducing the uncertainty. The remaining coeluted compounds (i.e., compounds circled as 1 and 2 in Fig. 4A, characteristic of the remaining olefins and sterenes) formed a different hump that was treated differently during the trimming process for quantification in order to obtain a smooth "panettone-shape" hump (when visualizing the plot in a three-dimensional way), as expected for a MOAH contamination. The combination of these two benefits in the 2D determination allowed to compensate for the effect of the operator interpretation on the subtraction extent. In the case of samples D and E, an inefficient removal of interferences can be hypothesized for UniUD as well. At the same time, the lower amount of MOAH obtained in the 2D analysis can again be explained by the support for removing the highly present interferences provided by the enhanced separation power (see Fig. 9). The same comparison between the 1D traces obtained in UniUD and GxABT and the 2D plots (original and trimmed) for all the other samples are reported in Supplementary Fig. S4.

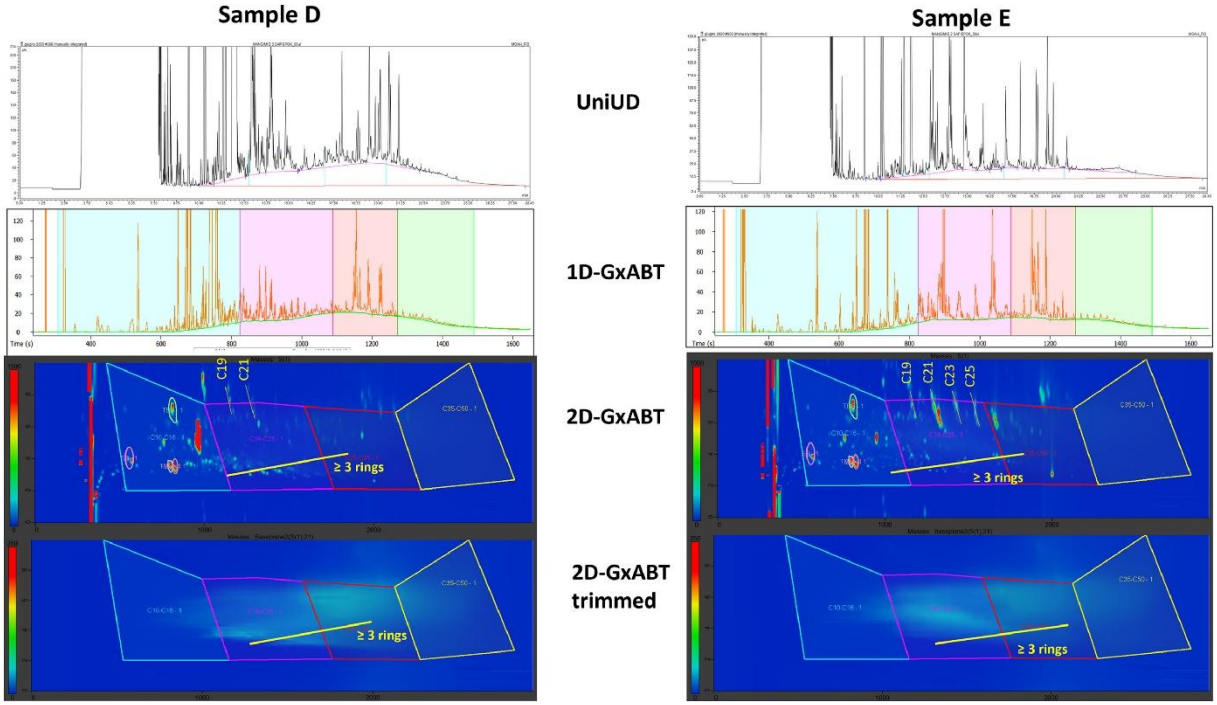

Fig. 9. Comparison of the LC-GC-FID obtained by UniUD and GxABT and the LC-GC×GC-FID plots before and after trimming for sample D and E.

Concerning the general MOAH profile of the feed, the first part of the trace is always characterized by the presence of three clusters of peaks, which were present also in the chromatogram obtained

Published in : Journal of Chromatography A (2022), vol. 1677, 463208
DOI: 10.1016/j.chroma.2022.463208
Status : Postprint (Author's version)

from the analysis of the fish fillet (circled in blue in Fig. 8). In the 2D chromatograms, these clusters appeared slightly above but partially overlapped with the monoaromatics. Probably they are interfering compounds that are endogenous to fishes and are vehiculated into the feed through the fish meal. As aforementioned, the identification is cumbersome because the similarities with the MS database are very low. Nevertheless, the position combined with the MS information suggested a possible identification as odd C-number chain dienes and trienes, possibly also branched, in the C_{19}-C_{25} range, with the predominance of the C_{19} and C_{21} (the presence of molecular ions 264, 262, 260 *m/z* characteristics of the $C_{19}H_{36}$, $C_{19}H_{34}$ and $C_{19}H_{32}$, respectively, were detected; the other groups presented previous fragments added of the +28 *m/z* ions related to the C_2H_4 addition). The presence of these compounds is highlighted in Fig. 9 and Supplementary Fig. S4 as C-number. The presence of some halogenated hydrocarbons slightly above the alkylbenzene was also depicted by the MS detector.

Looking at the MOAH distribution, it can be observed that the 1 and 2 ring compounds are the main MOAH present, although a significant amount of 3 rings and more was reported, ranging between 5 and 10%. The presence of such MOAH suggested the contamination with products deriving from petroleum after stream cracking, a treatment step usually related to the production of fuels, as for instance, marine fuels, to increase the octane number [49,50]. It can also be observed that the distinction between the compounds belonging to different rings number is not always sharp, but rather the space between the different rows is filled with other compounds which are related to the presence of refined petrogenic products [51]. In fact, refining may include hydrogenation, thus producing partially hydrogenated aromatic hydrocarbons (i.e., mixed aromatic and saturated rings), for instance, in the case of printing inks that may be used in the packaging of the feed product or its ingredients. The use of a 2D separation also allowed to take into account the contribution of the LABs to the overall contamination without the risk of including extra interferences, which were well-separated above the monoaromatic fraction. The results of the MOAH fractions in 2D are reported both applying the integration rule for MOAH, which says to trim all the running peaks on top of the hump (yellow bar in Fig. 7), but also considering the contribution of the LABs (lighter blue bar in Fig. 7). An increment ranging between 3.7 and 13.7% of the total MOAH amount was reported when considering the contribution of LABs, with the highest value for sample A and the lowest for sample D.

Finally, the 2D separation allowed to quantify the MOAH not only as total or according to the C-fraction requested by the JRC Guidance but also to quantify according to the number of rings, and more specifically, taking into account the more health-concerning 3–7 rings fraction in relation to the 1-2 rings [7]. Table 1 reports the quantification of the 1-2 ring and over 3 rings MOAH in each sample, along with the confirmation of the presence of benzothiophene, dibenzothiophene, and naphtobenzothiophene, markers of possible contamination with little refined oil [51]. The identification of the presence of these marker compounds was performed with the support of the mass filter feature explained in detail in [21]. In particular, fragment masses 134, 148, 162, 176, 190 *m/z* were used to visualize the benzothiophene coeluted with the diaromatics; fragment masses 184, 198, 212, 226, 240 *m/z* were considered to visualize the dibenzothiophene coeluted with triaromatic; while fragments 248, 262, 276, 290 *m/z* were used to highlight the presence of

Published in : Journal of Chromatography A (2022), vol. 1677, 463208
DOI: 10.1016/j.chroma.2022.463208
Status : Postprint (Author's version)

naphtobenzothiophene coeluted with the tetraromatics. An example of the use of the mass filters to support the identification is given in Fig. 10, while more details are provided in [21].

Table 1. MOAH content (mg/kg) according to the number of rings, i.e. 1-2 rings and ≥3 rings, along with the confirmation of the presence of benzothiophene, dibenzothiophene, and naphtobenzothiophene.

sample	1-2rings	≥3 rings	benzo-thiophene	dibenzo-thiophene	napthobenzo-thiophene
A	2.14	0.15	y	y	y
B	2.17	0.16	y	y	y
C	2.38	0.25	y	y	y
D	3.79	0.25	y	y	y
E	4.01	0.19	y	y	y
F	1.52	0.13	y	y	y
S	2.94	0.28	y	y	y

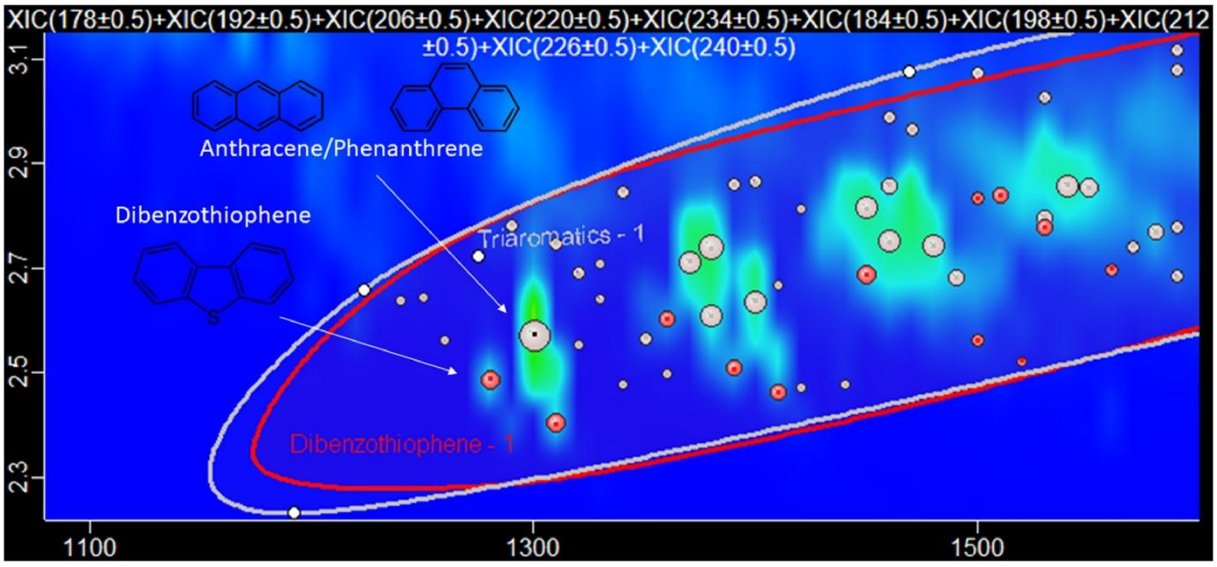

Fig. 10. Expansion of the ion extracted 2D plot in the dibenzothiophenes (in red) and triaromatics (in grey) area. The classification areas are depicted with the manually drawn ellipsis (red and grey) and the class to which every single component belongs is depicted by bubbles with the corresponding color.

Despite a superior characterization, thanks to the contribution of the data from the 2D separation in GC × GC, more investigations aimed at analyzing single feed ingredients and studying the possible transfer from the fish to the feed and from the feed to the fish (for farmed fish) are needed for a better elucidation of the possible sources of contamination and the different contribution to the overall level of MOSH and MOAH.

Published in : Journal of Chromatography A (2022), vol. 1677, 463208
DOI: 10.1016/j.chroma.2022.463208
Status : Postprint (Author's version)

4. Conclusion

The results obtained with the novel LC-GC × GC-ToFMS/FID platform (used both in 1D and 2D) were compared for the first time through a cross-laboratories comparison with the routinely accepted LC-GC-FID method. The same sample preparation method was applied for the analysis of commercial fish feed, exploiting the use of MAS followed by epoxidation for the MOAH fraction prior to the final LC-GC-FID or LC-GC × GC-ToFMS/FID determination. The integration and thus quantification of the LC-GC × GC-ToFMS/FID data was possible thanks to a novel algorithm recently explicitly developedfor 2D integration of MOSH and MOAH, while the data from the LC-GC-FID were handled with the traditional integration approach involving the manual removal of the riding peaks. The quantitative results were generally in good agreement both for MOSH and MOAH. The LC-GC × GC-ToFMS/FID allowed for a more robust removal of the interfering peaks, combining with the trimming of the hump the chromatographic separation in the 2D space. In fact, the remaining interferences were either chromatographically separated in the second dimension from the MOAH of interest or formed more defined peaks/narrow humps that were more easily recognized and subtracted from the overall contamination. Moreover, the GC × GC separation was exploited to report the data as 1–2 aromatic rings and 3–7 rings, as requested for toxicological evaluation by the EFSA [7]. Furthermore, the use of the MS allowed to support the interpretation of the remaining interferences, as well as to recognize the presence of a significant amount of LABs in the MOAH fraction of all the samples, otherwise simply subtracted from the integration of the hump in the C-fraction of interest.

These results are important to prove the reliability of the recently proposed LC-GC × GC-ToFMS/FID platform for routine application. In fact, it provides more robust results, supporting the critical sample preparation steps, a real challenge in MOSH and MOAH determination, along with an accurate quantification and more in-depth characterization of the contamination. The LC-GC × GC-ToFMS/FID platform simultaneously provides quantitative and confirmatory results, allowing to maximize the samples throughput.

Further studies would be needed, in particular analyzing single feed ingredients and possibly the fish feeded with the feed samples here analyzed, to evaluate the possible contribution of MOSH and MOAH transferred from the fish to the feed and from the feed to the fish (for farmed fish).

Declaration of Competing Interest

The authors have declared no conflict of interest.

Acknowledgments

This work is supported by Fonds de la Recherche Scientifique Belgique (FNRS) (CDR projects-MOHPlatform, J.0170.20). GP and GB thank LECO and Restek for their support. This article is based

upon work from the Sample Preparation Study Group and Network, supported by the Division of Analytical Chemistry of the European Chemical Society.

Supplementary materials

Supplementary material associated with this article can be found, in the online version, at doi: 10.1016/j.chroma.2022.463208.

References

1. International Agency for Research on Cancer (IARC), Mineral oils, untreated or mildly treated, IARC Monogr. Eval. Carcinog. Risks Hum. 100F (2012) 179–196.

2. K. Grob, A. Artho, M. Biedermann, J. Egli, Food Contamination by hydrocarbons from lubricating oils and release agents: determination by coupled LC-GC, Food Addit. Contam. 8 (1991) 437–446.

3. K. Grob, Could the Ukrainian sunflower oil contaminated with mineral oil wake up sleeping dogs? Eur. J. Lipid Sci. Technol. 110 (2008) 979–981, doi:10.1002/ejlt.200800234.

4. M. Biedermann, K. Grob, Is recycled newspaper suitable for food contact materials? Technical grade mineral oils from printing inks, Eur. Food Res. Technol. 230 (2010) 785–796, doi:10.1007/s00217-010-1223-9.

5. European Food Safety Authorithy (EFSA), Scientific opinion on mineral oil hydrocarbons in food, EFSA Journal. 10 (2012) 185, doi:10.2903/j.efsa.2012.2704.

6. European Commission, Commission recommendation (EU) 2017/84 of 16 January 2017 on the monitoring of mineral oil hydrocarbons in food and in materials and articles intended to come into contact with food, Off. J. Eur. Union L12 (2017) 95–96.

7. D. Arcella, K. Baert, M. Binaglia, Rapid risk assessment on the possible risk for public health due to the contamination of infant formula and follow-on formula by mineral oil aromatic hydrocarbons (MOAH), EFSA Support. Publ. 16 (2019), doi:10.2903/sp.efsa.2019.en-1741.

8. S. Bratinova, E. Hoekstra, European Commission Joint Research Center (JRC). Guidance on sampling, analysis and data reporting for the monitoring of mineral oil hydrocarbons in food and food contact materials. Publications Office of the European Union. (2019), doi:10.2760/208879.JRC115694.

9. L.W. Spack, G. Leszczyk, J. Varela, H. Simian, T. Gude, R.H. Stadler, Understanding the contamination of food with mineral oil: the need for a confirmatory analytical and procedural approach, Food Addit. Contam. Part A Chem. Anal. Control Expo. Risk Assess. 34 (2017) 1052–1071, doi:10.1080/19440049.2017. 1306655

Published in : Journal of Chromatography A (2022), vol. 1677, 463208
DOI: 10.1016/j.chroma.2022.463208
Status : Postprint (Author's version)

10. M. Biedermann, G. McCombie, K. Grob, O. Kappenstein, C. Hutzler, K. Pfaff, A. Luch, FID or MS for mineral oil analysis? J. Verbraucherschutz Lebensm. 12 (2017) 363–365, doi:10.1007/s00003-017-1127-8.

11. S. Bratinova, E. Hoekstra, H. Emons, C. Hutzler, O. Kappenstein, M. Biedermann, G. McCombie, The reliability of MOSH/MOAH data: a comment on a recently published article, J. Verbraucherschutz Lebensm. (2020) 2–4, doi:10.1007/s00003-020-01287-w.

12. A. Hochegger, S. Moret, L. Geurt, T. Gude, E. Meitner, B. Mertens, S. O'Hagan, F. Poças, T. Simat, G. Purcaro, Mineral oil risk assessment : knowledge gaps and roadmap. Outcome of a multi-stakeholders workshop, Trends Food Sci Technol. 113 (2021) 151–166, doi:10.1016/j.tifs.2021.03.021.

13. M. Biedermann, K. Fiselier, K. Grob, Aromatic hydrocarbons of mineral oil origin in foods: method for determining the total concentration and first result, J. Agric. Food Chem. 57 (2009) 8711–8721, doi:10.1021/jf901375e.

14. M. Biedermann, C. Munoz, K. Grob, Update of on-line coupled liquid chromatography – gas chromatography for the analysis of mineral oil hydrocarbons in foods and cosmetics, J. Chromatogr. A 1521 (2017) 140–149, doi:10.1016/j. chroma.2017.09.028.

15. L. Barp, G. Purcaro, S. Moret, L.S. Conte, A high-sample-throughput LC-GC method for mineral oil determination, J. Sep. Sci. 36 (2013) 3135–3139, doi:10.1002/jssc.201300114.

16. M. Biedermann, K. Grob, On-line coupled high performance liquid chromatography-gas chromatography for the analysis of contamination by mineral oil. Part 1: method of analysis, J. Chromatogr. A 1255 (2012) 56–75, doi:10.1016/j.chroma.2012.05.095.

17. M. Biedermann, L. Barp, C. Kornauth, T. Würger, M. Rudas, A. Reiner, N. Concin, K. Grob, Mineral oil in human tissues, Part II: characterization of the accu-mulated hydrocarbons by comprehensive two-dimensional gas chromatography, Sci. Total Environ. 506–507 (2015) 644–655, doi:10.1016/j.scitotenv.2014.07.038.

18. G. McCombie, K. Hötzer, J. Daniel, M. Biedermann, A. Eicher, K. Grob, Compliance work for polyolefins in food contact: results of an official control campaign, Food Control 59 (2016) 793–800, doi:10.1016/j.foodcont.2015.06.058.

19. G. Purcaro, P.Q. Tranchida, L. Barp, S. Moret, L.S. Conte, L. Mondello, Detailed elucidation of hydrocarbon contamination in food products by using solid-phase extraction and comprehensive gas chromatography with dual detection, Anal. Chim. Acta 773 (2013) 97–104, doi:10.1016/j.aca.2013.03.002.

20. M. Zoccali, P.Q. Tranchida, L. Mondello, On-line liquid chromatography-comprehensive two dimensional gas chromatography with dual detection for the analysis of mineral oil and synthetic hydrocarbons in cosmetic lip care products, Anal. Chim. Acta 1048 (2019) 221–226, doi:10.1016/j.aca.2018.10.069.

Published in : Journal of Chromatography A (2022), vol. 1677, 463208
DOI: 10.1016/j.chroma.2022.463208
Status : Postprint (Author's version)

21. S. Panto', M. Collard, G. Purcaro, Comprehensive gas chromatography coupled to simultaneous dual detection (TOF-MS/FID) as a confirmatory method for MOSH and MOAH determination in food, Curr. Trend Mass Spectrom. 18 (2020) 1–6.

22. M. Biedermann, K. Grob, Comprehensive two-dimensional GC after HPLC pre-separation for the characterization of aromatic hydrocarbons of mineral oil origin in contaminated sunflower oil, J. Sep. Sci. 32 (2009) 3726–3737, doi:10.1002/jssc.200900366.

23. K. Grob, Mineral oil hydrocarbons in food: a review, Food Addit. Contam. Part A Chem. Anal. Control Expo. Risk Assess. 35 (2018) 1845–1860, doi:10.1080/19440049.2018.1488185.

24. S. Weber, K. Schrag, G. Mildau, T. Kuballa, S.G. Walch, D.W. Lachenmeier, Analytical methods for the determination of mineral oil saturated hydrocarbons (MOSH) and mineral oil aromatic hydrocarbons (MOAH)—a short review, Anal. Chem. Insights 13 (2018), doi:10.1177/1177390118777757.

25. S. Moret, C. Conchione, A. Srbinovska, P. Lucci, Microwave-based technique for fast and reliable extraction of organic contaminants from food, with a special focus on hydrocarbon contaminants, Foods 8 (2019) 503, doi:10.3390/foods8100503.

26. N. Sdrigotti, M. Collard, G. Purcaro, Evolution of hyphenated techniques for mineral oil analysis, J. Sep. Sci. 44 (2021) 464–482, doi:10.1002/jssc.202000901.

27. S. Moret, M. Scolaro, L. Barp, G. Purcaro, L.S. Conte, Microwave assisted saponification (MAS) followed by on-line liquid chromatography (LC)-gas chromatography (GC) for high-throughput and high-sensitivity determination of mineral oil in different cereal-based foodstuffs, Food Chem. 196 (2016) 50–57, doi:10.1016/j.foodchem.2015.09.032.

28. A. Srbinovska, C. Conchione, P. Lucci, S. Moret, On-line HP(LC)-GC-FID determination of hydrocarbon contaminants in fresh and packaged fish and fish products manuscript, J. AOAC Int. 104 (2021) 267–273.

29. O. Mironov, T. Shchekaturina, I. Tsimbal, Saturated hydrocarbons in marine organisms, Mar. Ecol. Prog. Ser. 5 (1981) 303–309, doi:10.3354/meps005303.

30. S. Moret, K. Grob, L.S. Conte, Mineral oil polyaromatic hydrocarbons in foods, e.g. from jute bags, by on-line LC-solvent evaporation (SE)-LC-GC-FID, Z Lebensm. Unters. Forsch. A 204 (1997) 241–246.

31. A .M. Booth, P.A . Sutton, C.A . Lewis, A .C. Lewis, A . Scarlett, W. Chau, J. Widdows, S.J. Rowland, Unresolved complex mixtures of aromatic hydrocarbons: thousands of overlooked persistent, bioaccumulative, and toxic contaminants in mussels, Environ. Sci. Technol. 41 (2007) 457–464, doi:10.1021/es0615829.

32. N. Cappelletti, E. Speranza, L. Tatone, M. Astoviza, M.C. Migoya, J.C. Colombo, Bioaccumulation of dioxin-like PCBs and PBDEs by detritus-feeding fish in the Rio de la Plata estuary, Argentina, Environ. Sci. Pollut. Res. 22 (2015) 7093– 7100, doi:10.1007/s11356-014-3935-z.

Published in : Journal of Chromatography A (2022), vol. 1677, 463208
DOI: 10.1016/j.chroma.2022.463208
Status : Postprint (Author's version)

33. A. Van Heyst, M. Vanlancker, J. Vercammen, K. Van den Houwe, B. Mertens, M. Elskens, E. Van Hoeck, Analysis of mineral oil in food: results of a Belgian market survey, Food Addit. Contam. Part A Chem. Anal. Control Expo. Risk As-sess. 35 (2018) 2062–2075, doi:10.1080/19440049.2018.1512758.

34. G. Bauwens, S. Pantó, G. Purcaro, Mineral oil saturated and aromatic hydrocar-bons quantification: mono- and two-dimensional approaches, J. Chromatogr. A. 1643 (2021) 462044, doi:10.1016/j.chroma.2021.462044.

35. [CEN] European Committee for Standardization European standard, Foodstuffs - Vegetable oils and foodstuff on basis of vegetable oils - Determination of mineral oil saturated hydrocarbons (MOSH) and mineral oil aromatic hydrocarbons (MOAH) with on-line HPLC-GC-FID analysis, (EN) 16995:2017.

36. M. Nestola, T.C. Schmidt, Determination of mineral oil aromatic hydrocarbons in edible oils and fats by online liquid chromatography–gas chromatography– flame ionization detection – evaluation of automated removal strategies for biogenic olefins, J. Chromatogr. A 1505 (2017) 69–76, doi:10.1016/j.chroma.2017.05.035.

37. M. Biedermann, K. Grob, Memory effects with the on-column interface for on-line coupled high performance liquid chromatography-gas chromatography: the Y-interface, J. Chromatogr. A 1216 (2009) 8652–8658, doi:10.1016/j.chroma.2009.10.039.

38. L. Menegoz Ursol, C. Conchione, A. Srbinovska, S. Moret, Optimization and validation of microwave-assisted saponification (MAS) followed by epoxidation for high-sensitivity determination of mineral oil aromatic hydrocarbons (MOAH) in extra virgin olive oil, Food Chem. 370 (2022) 130966, doi:10.1016/ j.foodchem.2021.130966.

39. T. Populin, M. Biedermann, K. Grob, S. Moret, L. Conte, Relative hopane content confirming the mineral origin of hydrocarbons contaminating foods and human milk, Food Addit. Contam. 21 (2004) 893–904, doi:10.1080/02652030400001164.

40. M. Zoccali, L. Barp, M. Beccaria, D. Sciarrone, G. Purcaro, L. Mondello, Improvement of mineral oil saturated and aromatic hydrocarbons determination in edible oil by liquid-liquid-gas chromatography with dual detection, J. Sep. Sci. 39 (2016) 623–631, doi:10.1002/jssc.201501247.

41. M. Biedermann, C. Munoz, K. Grob, Epoxidation for the analysis of the mineral oil aromatic hydrocarbons in food. An update, J. Chromatogr. A 1624 (2020) 461236, doi:10.1016/j.chroma.2020.461236.

42. S. Tsutsumi, Y. Yamaguchi, I. Nishida, K. Akiyama, M.P. Zakaria, H. Takada, Alkylbenzenes in mussels from South and South East Asian coasts as a molecular tool to assess sewage impact, Mar. Pollut. Bull. 45 (2002) 325–331, doi:10.1016/s0025-326x(02)00151-0.

43. P.C. Hartmann, J.G. Quinn, J.W. King, S. Tsutsumi, H. Takada, Intercalibration of LABs in marine sediment SRM 1941A and their application as a molecular marker in Narragansett bay sediments, Environ. Sci. Technol. 34(2000)900–906, doi:10.1021/es990798q.

Published in : Journal of Chromatography A (2022), vol. 1677, 463208
DOI: 10.1016/j.chroma.2022.463208
Status : Postprint (Author's version)

44. C. Conchione, C. Picon, R. Bortolomeazzi, S. Moret, Hydrocarbon contaminants in pizza boxes from the Italian market, Food Packag. Shelf Life 25 (2020) 100535, doi:10.1016/j.fpsl.2020.100535.

45. M.I. Venkatesan, T. Northrup, C.R. Phillips, Determination of linear alkylbenzenes in fish tissue by gel permeation chromatography and gas chromatography-mass spectrometry, J. Chromatogr. A 942 (2002) 223–230, doi:10.1016/S0021-9673(01)01400-5.

46. R.P. Eganhouse, E.C. Ruth, I.R. Kaplan, Determination of long-chain alkylbenzenes in environmental samples by argentation thin-layer chromatography/high-resolution gas chromatography and gas chromatography/mass spectrometry, Anal. Chem. 55 (1983) 2120–2126, doi:10.1021/ac00263a028.

47. B. Aurela, T. Ohra-aho, L. Söderhjelm, Migration of alkylbenzenes from packaging into food and Tenax, Packag. Technol. Sci. 14 (2001) 71–77, doi:10.1002/pts.534.

48. C.R. Phillips, M.I. Venkatesan, T. Lin, Linear alkylbenzenes in muscle tissues of white croaker near a large ocean outfall in Southern California, USA, Environ. Toxicol. Chem. 20 (2001) 231–238, doi:10.1002/etc.5620200202.

49. M. Geerts, N. Ristic, M. Djokic, S. Ukkandath Aravindakshan, G.B. Marin, K.M. Van Geem, Crude to olefins: effect of feedstock composition on coke formation in a bench-scale steam cracking furnace, Ind. Eng. Chem. Res. 59 (2020) 2849–2859, doi:10.1021/acs.iecr.9b06702.

50. K. Van Geem, G.B. Reyniers, M.F. Marin, Challenges of modeling steam cracking of heavy feedstocks, Oil Gas Sci. Technol. 63 (2008) 79–94, doi:10.2516/ogst.

51. M. Biedermann, K. Grob, Comprehensive two-dimensional gas chromatography for characterizing mineral oils in foods and distinguishing them from synthetic hydrocarbons, J. Chromatogr. A 1375 (2015) 146–153, doi:10.1016/j.chroma.2014.11.064.